JOURNAL OF MATERIALS SCIENCE 31 (1996) 357–362

Time-domain dielectric relaxation in polyamide 6, poly(vinyl chloride), ethylene-vinyl acetate copolymer and poly(vinylidene fluoride)

M. SAFARI ARDI, D. H. McQUEEN*
*Department of Polymeric and Textile Materials, and *Chalmers Innovation Centre, Chalmers University of Technology 412 96 Gothenburg, Sweden*

The time-domain dielectric responses of polyamide 6 (PA6), poly(vinyl chloride) (PVC), ethylene-vinyl acetate copolymer (EVA) and poly(vinylidene fluoride) (PVDF) to a voltage step were measured at different temperatures. From the variation of the sample capacitance, C, with time, the ratio $F_d/\Delta C$ was determined, where $F_d = (dC/d\ln t)_{max}$ is the maximum (inflexion) slope of the capacitance versus log(time) dipole response curve, and ΔC is the difference between the initial and the extrapolated equilibrium capacitance values. A modified Kohlrausch–Williams–Watts (stretched exponential) function provided a good fit to the measured $C(t)$ data. For low temperatures, typically below $-20\,^{\circ}C$, $F_d/\Delta C$, is about 0.1, characteristic of highly cooperative relaxation, while at higher temperatures the ratio approaches $1/e$, characteristic of nearly independent (Maxwellian) relaxation. This is in contrast to corresponding analyses of mechanical relaxation in solids for which the constant is almost always near 0.1 at room temperature.

1. Introduction

In previous articles [1, 2] we analysed the time-domain dielectric behaviour of poly(methyl methacrylate) (PMMA) and nitrile butadiene rubber (NBR) with the aim of establishing possible connections with the kinetics of stress relaxation. The starting point of the comparison was a relation characterizing the extension of stress relaxation curves along the logarithmic time axis [3]

$$F = -(d\sigma/d\ln t)_{max} = (0.1 \pm 0.01)\Delta\sigma \quad (1)$$

where F denotes the maximum (inflexion) slope of the stress (σ)–log time (t) diagrams, and $\Delta\sigma$ is the total stress decrease in the relaxation process. The constant (0.1 ± 0.01) is an empirical result characterizing mechanical relaxation in solids.

Normally, for mechanical relaxation in solid polymers, the inflexion region is rectilinear over several decades of time. Deviations from the behaviour described by Equation 1 are observed at temperatures near thermal transition regions where a distinct increase of the constant of proportionality in Equation 1 is noted. The bulk of experimental data supporting the validity of this empirical finding for mechanical relaxation relates to room temperature. Equation 1 describes the behaviour not only of many polymers but also that of many metals and other solids [3].

When comparing Equation 1 with the observed time-domain dielectric relaxation behaviour of PMMA, good agreement is found at temperatures between about -10° and $+32\,^{\circ}C$ [1], the normalized inflexion slope $F_d/\Delta C$, showing a slow monotonic increase with temperature. The quantity ΔC is the total increase in capacitance which can be associated with dipole reorientation and F_d denotes the inflexion slope of the capacitance–log time diagrams for the dielectric case.

For NBR, numerical agreement with Equation 1 was limited to temperatures below $-25\,^{\circ}C$ [1]; at higher temperatures the slope $F_d/\Delta C$ was significantly higher.

The aim of this paper is to present time-domain dielectric data for four other polymers and to discuss their bearing on Equation 1. The polymers included in this study are polyamide 6, PA6, poly(vinyl chloride), PVC, an ethylene-vinyl acetate copolymer, EVA and poly(vinylidene fluoride), PVDF. All these materials have sufficient degrees of polarity to allow charging experiments to be carried out with fair accuracy.

2. Experimental procedure

The measuring principle and the experimental set-up (Time-Domain Dielectric Spectrometer, IMASS Inc., Hingham, MA, USA) have been described previously [1]. The method used is based on applying a voltage step to the sample held between the plates of a capacitor. The equipment records the increase of the capacitance with time, $C(t)$.

Owing to intrinsic conductivity, $C(t)$ did not reach an equilibrium value, as could be expected for a dipole reorientation process, but continued to increase at longer measuring times. The relative contributions of the dipole reorientation and the conductivity are

0022–2461

different in different materials. They also depend on the temperature. A simple graphical method, described previously [1], was used to estimate the dipole contribution which is the subject of the present study.

The measurements were carried out after the samples and the reference capacitors had been purged with dry nitrogen for sufficient periods of time (2 h for the references and more than 24 h for the samples). The drying procedure was especially important for the PA6 sample, which exhibited a relatively high degree of hygroscopicity. PA6 was purged with dry nitrogen for 12 h at 140 °C, PVC at 60 °C, EVA at 30 °C, and PVDF at 120 °C and then cooled down slowly for 12 h. In all experiments, the purging with dry nitrogen went on for the whole duration of the measurement.

For PA6, the first measurements were made while the temperature increased from + 22.6 °C to + 70 °C, thus passing the T_g level of this polymer (+ 50.5 °C). Then the sample was allowed to cool slowly to room temperature (1 °C min^{-1}), whereafter measurements were performed during cooling (1 °C min^{-1}) from + 20 °C to − 60 °C. With PVC, the measuring sequence covered the temperature ranges room temperature to + 60 °C and room temperature to − 50 °C. The charging behaviour of the EVA samples was recorded between room temperature and − 40 °C. Finally, for PVDF the first measurements were for room temperature to 110 °C. This was followed by a cooling procedure as above, and the range + 20 to − 45 °C was then covered.

3. Materials

PA6 (B3, BASF) was injection moulded into plaques (100 mm × 100 mm × 3.35 mm) at 230 °C. Its T_g value (DSC, cooling rate 10 °C min^{-1}) was + 50.5 °C. The circular samples had an area of 15.27 cm^2, corresponding to a geometric capacitance of 4.0 pF as calculated from $C_g = \varepsilon_0 A/d$ (ε_0 being the permittivity of free space, A the area and d the thickness of the sample).

PVC was obtained as 2.2 mm thick calendered and compression-moulded sheet (Norsk Hydro Plast AB, Stenungsund, Sweden). Its composition was 100 parts suspension grade PVC (Norvinyl S658), 1 part calcium stearate and 3 parts Naftovin T3. The T_g value (DSC, cooling rate 3 °C min^{-1}) was 88 °C. The M_n and M_w values were 3.5×10^4 and 9.7×10^4, respectively; the intrinsic viscosity was 0.86. The PVC sample had an area of 15.1 cm^2, corresponding to a geometric capacitance of 6.1 pF.

The EVA copolymer (EVA28-150 from Atochem) contained 28% by weight of vinyl acetate. The material was compression moulded into plaques with dimensions 150 mm × 100 mm × 3 mm at 100 °C for 10 min. The pressure was 2.6 MPa. The material was then allowed to cool slowly until it solidified under pressure. Its M_n and M_w values were 1.2×10^4 and 1.1×10^5, respectively. The T_g value (DSC, cooling rate 10 °C min^{-1}) was − 27 °C. The EVA sample had an area of 15.27 cm^2, which gave a geometric capacitance of 4.5 pF.

The PVDF sample was obtained as a film (100 mm × 100 mm × 0.8 mm) from Goodfellow Cambridge Limited, UK. A sample cut from the above film had an area of 16.40 cm^2, which gave a geometric capacitance of 18.1 pF. Its T_g value (DSC, cooling rate 10 °C min^{-1}) was − 34.7 °C.

4. Analysis of the experimental curves

Before presenting the results, some remarks on the evaluation of the $C(\log t)$ diagrams are appropriate. Following the application of a voltage step to the sample, the sample capacitance increases in a complex way determined by the polarization mechanism in progress and also by the contribution of the conductivity. The theoretical background necessary for a satisfactory quantitative description of phenomena of this kind is rather weak. Therefore, a simple method has been used to extract the information which can be used in Equation 1. Typically, the shapes of the $C(\log t)$ curves to be analysed in the present case include a sigmoidal part corresponding to dipole reorientation at shorter times followed by a nearly linear part corresponding to electrical conduction, probably ionic. In the absence of the conductivity contribution the sigmoidal dipole region would end in a horizontal plateau. However, the conductivity part of the charging process obscures the final portion of the dipole region, thus complicating the evaluation of its characteristic parameters. In some cases the conductivity part becomes so dominant that the dipole region cannot be separated from the conductivity part.

The simplest method of analysing the dipole part of the $C(\log t)$ diagrams is to separate it from the conductivity contribution by graphical extrapolation. This method relies on the fact that the inflexion region of the dipole process is nearly linear over a relatively large interval of $\log t$, thus allowing a straight line tangent to the inflexion to be drawn. This gives $F_d = (\mathrm{d}C/\mathrm{d}\ln t)_{max}$. Also the initial part of the conductivity process, coinciding with the approach to equilibrium of the dipole movement, can often be approximated by a straight line. The intercept of these two lines gives ΔC, which is the contribution of the dipole process to the total capacitance increase.

In accordance with the above, the response function, $R(t)$, can be written [4, 5]

$$R(t) = R_i + R_r[1 - \varphi(t)] + R_{lt}\, t \qquad (2)$$

where R_i is the instantaneous part of $R(t)$ (at $t = 0$), R_r is its dipole relaxation part with $\varphi(t)$ the relaxation function, and $R_{lt}\, t$ denotes the increase in R at long times due to conductivity (assumed linear in the time).

The relaxation function, $\varphi(t)$, can be expressed analytically in a number of ways, there being no single most satisfactory derivation of it at the present time. A commonly used form is the stretched exponential or Kohlrausch–Williams–Watts (KWW) function, $\exp(-t/\tau)^\beta$ where β is typically in the interval $0 < \beta < 1$. For such a relaxation function one readily finds $F_d/\Delta C = \beta/e$.

As in previous work [1], a slightly modified KWW function is used to depict the time dependence of C within the dipole response region

$$[C(t) - C_0]/C_0 = \Delta C/C_0 \exp[-(t + t_c)^\beta/\tau^\beta + t_c^\beta/\tau^\beta] \quad (3)$$

The correction t_c improves the quality of fitting in the initial part of the dipole process. This is related to the finite rise time of the voltage step (3 μs) applied across the sample and also to the time needed by the computer to produce the first capacitance reading (10 μs). Although they are of the same order of magnitude, there is no quantitative relation between these two quantities and the correction t_c.

For the modified KWW expression, Equation 3, the expression for the maximum slope is

$$F_d/\Delta C = (\beta/e)\exp(t_c/\tau)^\beta \quad (4)$$

Normally, the correction factor $\exp(t_c/\tau)^\beta$ is of minor importance, because t_c is usually much less than τ. However, in some cases, $\exp(t_c/\tau)^\beta$ is as much as 1.5.

In the following, F_d and ΔC were first determined graphically. Then that value of ΔC was used in Equation 3 to determine best fit β, τ and t_c to the measured data. $F_d/\Delta C$ was then evaluated from Equation 4. For details of the evaluation procedure the reader is referred to a previous publication [1].

5. Results

5.1. PA6

Fig. 1 shows the charging behaviour of PA6 between room temperature and 70 °C. As can be seen, the $C(\log t)$ diagrams are dominated by the conductivity contribution. Only at the lowest temperature (+ 22.6 °C, + 30 °C) can the dipole process be isolated with a fair degree of certainty and fitted to the unmodified KWW function with $t_c = 0$. At + 40 °C the dipole contribution is smaller and it disappears entirely at high temperatures, that is to say above the T_g level of this material (around + 50 °C). On the other hand, at lower temperatures the separation of the dipole contribution from that of the conductivity could be carried out relatively easily. Fig. 2 shows results for + 20, − 20, and − 30 °C. The solid lines correspond to the modified KWW function. At − 40 °C and below two relaxation processes could be extracted from the $C(\log t)$ curves. The corresponding frequency domain curves reveal the two relaxation processes as indicated below in Fig. 4. It is seen that a new relaxation process begins to be significant at − 40 °C and below. Because this makes evaluation of F_d significantly more difficult, we did not calculate the normalized slopes for the two simultaneous relaxation processes.

Fig. 3a shows the inflexion slope of the $C(\log t)$ curves for PA6 normalized by the capacity change ΔC due to dipole relaxation for temperatures between − 30 °C and + 30 °C. The crosses are normalized inflexion slopes as calculated by the graphical method, while the circles are corresponding slopes calculated from the values of β according to Equation 3 and the formula $F_d/\Delta C$ (Equation 4) with ΔC from the graphical method. The two estimates of the normalized inflexion slopes are in good agreement.

The results for PA6 shown in Fig. 3a might be summarized as follows. For the lowest temperature, − 30 °C, the normalized slope is about 0.1, while for the higher temperatures, from − 20 °C to + 30 °C it increases significantly.

Fig. 4 shows the β relaxation peaks obtained from the time-domain data by suitable transforms available in the computer connected to the measuring equipment. By plotting the peak frequencies versus the inverse of the corresponding temperatures, an activation energy of 14.5 kcal mol^{-1} (4.187 cal equal 1 Joule) was obtained for this process in agreement with results obtained by McCrum *et al.* [5].

5.2. PVC

The charging behaviour of rigid PVC at lower temperatures (− 20, − 30, − 40 °C) is illustrated in Fig. 5.

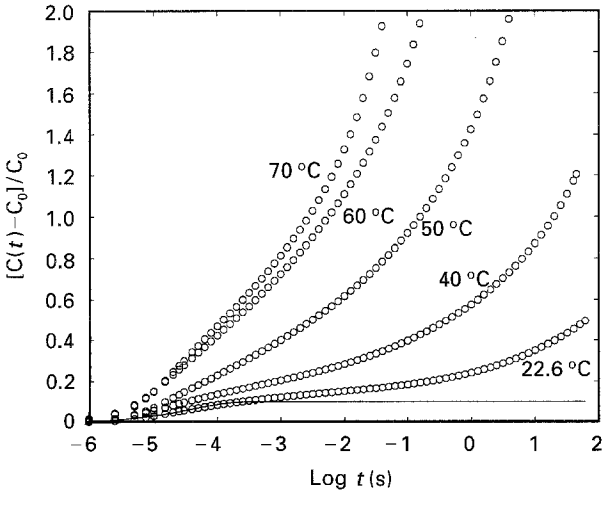

Figure 1 Normalized $C(\log t)$ curves for PA6 at 22.6 °C (C_0 = 15.6222 pF, $t_c = 0$), 40 °C (C_0 = 16.4116 pF), 50 °C (C_0 = 19.0675 pF), 60 °C (C_0 = 22.8171 pF), and 70 °C (C_0 = 32.0093 pF). (—) Curve relating to the dipole region, calculated using Equation 3 with C_∞ obtained by graphical extrapolation.

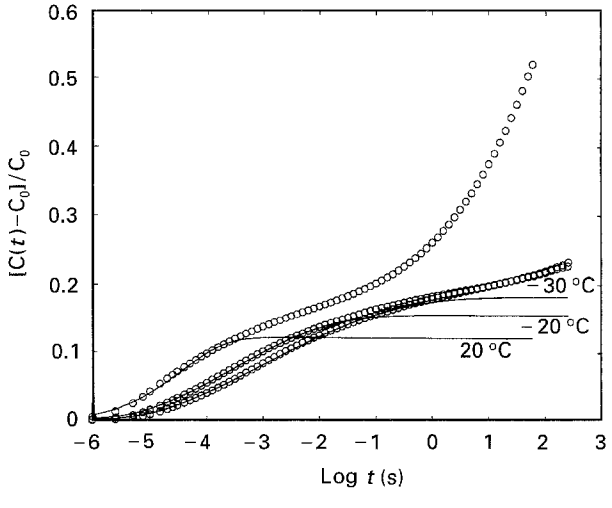

Figure 2 Normalized $C(\log t)$ curves for PA6 at 20 °C (C_0 = 15.4606 pF, $t_c = 10^{-6}$), − 20 °C (C_0 = 14.0840 pF, $t_c = 5 \times 10^{-6}$), and − 30 °C (C_0 = 13.9406 pF, $t_c = 9 \times 10^{-6}$). (—) Curves obtained using Equation 3 and graphically extrapolated C_∞ values separating the dipole and conduction regions.

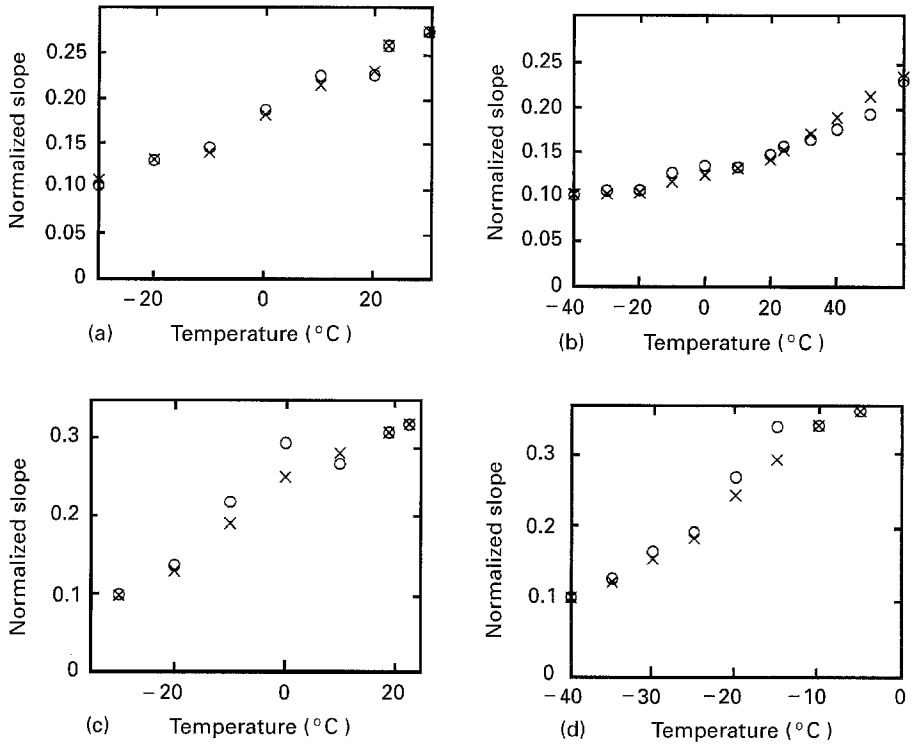

Figure 3 The temperature dependence of the normalized slope obtained by both (×) the graphical method and (○) the modified KWW function, for (a) PA6, (b) PVC, (c) EVA, and (d) PVDF.

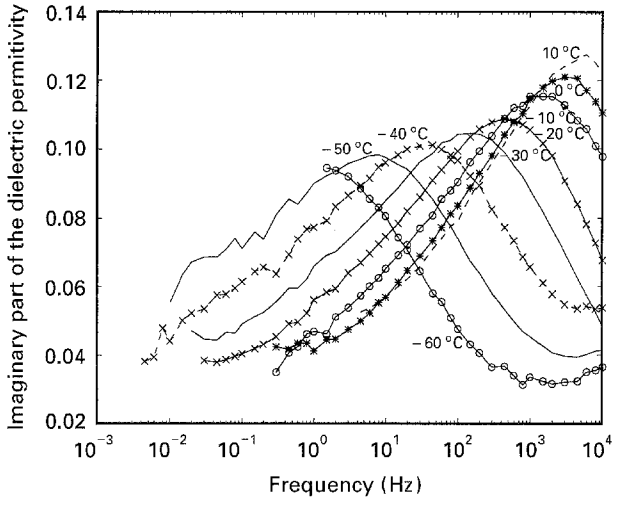

Figure 4 The variation of the imaginary part of the dielectric permittivity with frequency for PA6 between + 10 and − 60 °C. These data have been obtained by computer conversion of the time-domain results using a programme provided with the spectrometer used.

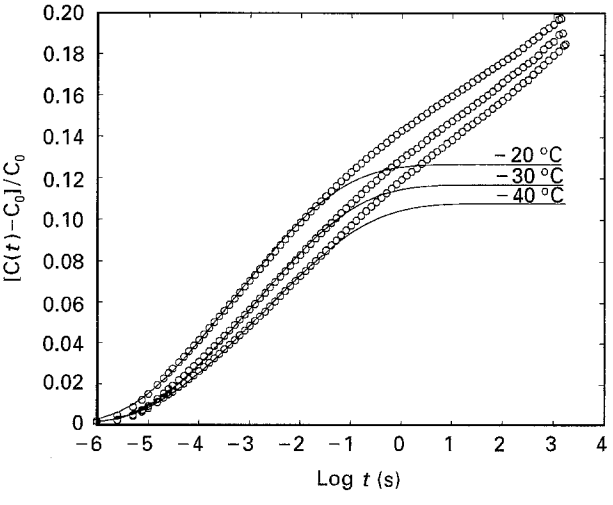

Figure 5 Normalized $C(\log t)$ curves for rigid PVC at − 20 °C ($C_0 = 18.2979$ pF, $t_c = 3 \times 10^{-6}$), − 30 °C ($C_0 = 18.1901$ pF, $t_c = 5 \times 10^{-6}$), and − 40 °C ($C_0 = 18.0534$ pF, $t_c = 4 \times 10^{-6}$). (—) Curves calculated using the same procedure as with PA6.

In this temperature range the contribution of the dipole reorientation can be separated from that of the conductivity. At − 50 °C the normalized slope was not calculated because it was not possible to extract a relaxation process from the $C(\log t)$ curve.

Fig. 3b shows the inflexion slopes of the $C(\log t)$ curves for PVC normalized by the ΔC corresponding to dipole relaxation for temperatures between − 40 °C and + 60 °C in exactly the same way as for PA6. Again, the two methods of determining the normalized inflexion slopes are in good agreement. The data might be summarized as follows. For lower temperatures (between − 40 °C and about − 15 °C) the normalized inflexion slope is near 0.1. For higher temperatures it increases significantly with temperature.

By transforming the time-domain data in the same way as previously, the dependence of the imaginary part of the dielectric constant diagrams on the frequency was obtained. From this the activation energy of the loss mechanism was calculated to be 14 kcal mol^{-1}, in agreement with results published by McCrum *et al.* [5].

5.3. EVA

With EVA, the dipole contributions to the charging curves were easily separated from those of the

conductivity. In Fig. 6 the solid lines calculated using Equation 3 fit the data well. For the curves at + 23.7 and + 19 °C, good fits were obtained with $t_c = 0$. At lower temperatures (− 10, − 20, − 30 °C) the dipole contribution becomes more pronounced and even more easily handled. However, at − 40 °C and below no dipole contribution could be extracted from the curves because a monotonic increase in the $C(\log t)$ curves was observed.

The corresponding normalized inflexion slope data for EVA are shown in Fig. 3c. The discrepancy between the two evaluation methods is largest for − 10 and 0 °C. The normalized inflexion slope is near 0.1 at the lowest temperatures but increases quickly as the temperature is raised. An activation energy of 47 kcal mol^{-1} was calculated for EVA using the data in Fig. 7.

5.4. PVDF

The charging behaviour of PVDF for selected temperatures is shown in Fig. 8. As seen, at − 45 and − 50 °C a steady increase of the $C(\log t)$ is observed. We could not extract the dipole part of the response at these temperatures. The solid lines are the results of fitting Equation 3 to the experimental values. At − 10 and − 5 °C, the data could be fit well with $t_c = 0$.

Fig. 3d shows normalized inflexion slope versus temperature data for PVDF, just as previously. Here the agreement between the two evaluation methods is good, except for the points at − 15 and − 20 °C. The normalized inflexion slope increases steadily from about 0.1 at − 40 °C as the temperature is raised.

At − 5 °C and above (up to 20 °C) two relaxation processes are present in the $C(\log t)$ diagrams. This makes evaluation of the normalized slope of the faster relaxation (which is the relevant one here) by the graphical method somewhat uncertain, as the slower relaxation is superimposed on it and can cause a distortion. The normalized slope found by the graphical method, 0.36, can thus be a little too high, for this reason. The second relaxation at − 5 °C at longer times was not evaluated because the conduction part was too short to allow use of the graphical method. Also, this longer relaxation is not the same one as was evaluated at the lower temperatures.

At 0 °C, again two relaxation processes are present. Here the faster relaxation is so fast (of the order of 10 μs) that the instrument response (also of the order of 10 μs) cannot provide dependable values for enough of the relaxation time to allow accurate extraction of the normalized slope. This is in addition to the fact that the longer relaxation process is superimposed on the shorter one. Thus the normalized slope of the relaxation process at 0 °C is not included in Fig. 3d.

Fig. 9 shows both the α_c (lower frequencies) and the α_a (higher frequencies) relaxation peaks. The α_a relaxation (also called β relaxation) is associated with segmental motion in the amorphous regions. The α_c relaxation (also called α relaxation) is associated with molecular motion in the crystalline regions. A calculation of the activation energy yielded a value of 23 kcal mol^{-1} for the α_c relaxation in the range

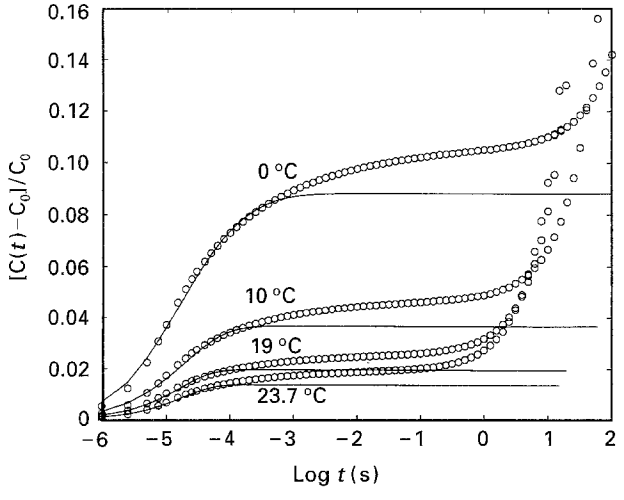

Figure 6 Normalized $C(\log t)$ curves for EVA at + 23.7 °C (C_0 = 15.8548 pF, $t_c = 0$), + 19 °C (C_0 = 15.7962 pF, $t_c = 0$), + 10 °C (C_0 = 15.5853 pF, $t_c = 10^{-6}$), and 0 °C (C_0 = 14.8415 pF, $t_c = 4 \times 10^{-6}$). (—) Curves relating to the dipole region, calculated using Equation 3 with C_∞ obtained by graphical extrapolation.

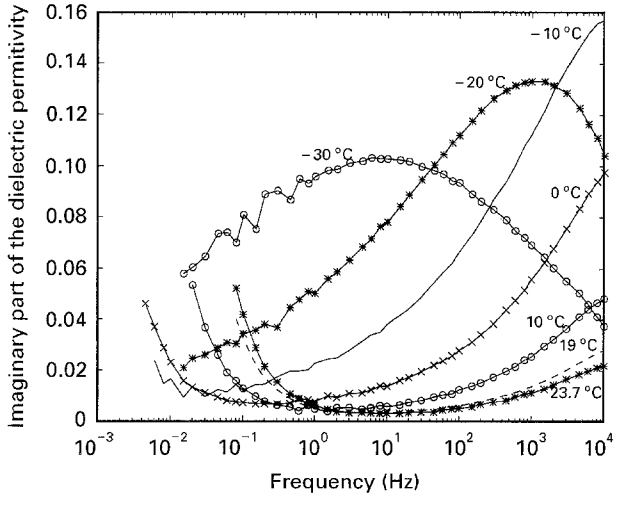

Figure 7 The variation of the imaginary part of the dielectric permittivity with frequency for EVA between + 23.7 and − 30 °C, cf. Fig. 4.

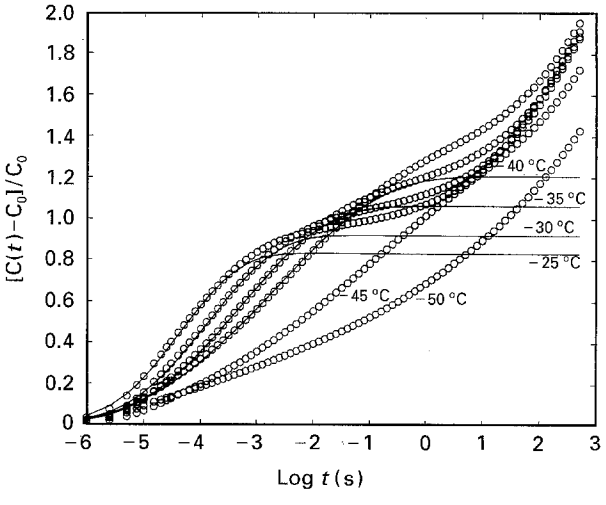

Figure 8 Normalized $C(\log t)$ curves for PVDF at − 25 °C (C_0 = 79.2383 pF, $t_c = 3 \times 10^{-6}$), − 30 °C (C_0 = 75.0391 pF, $t_c = 3 \times 10^{-6}$), − 35 °C (C_0 = 69.5703 pF, $t_c = 3 \times 10^{-6}$), and − 40 °C (C_0 = 62.9297 pF, $t_c = 1.5 \times 10^{-6}$). (—) Curves calculated using the same procedure as with PA6.

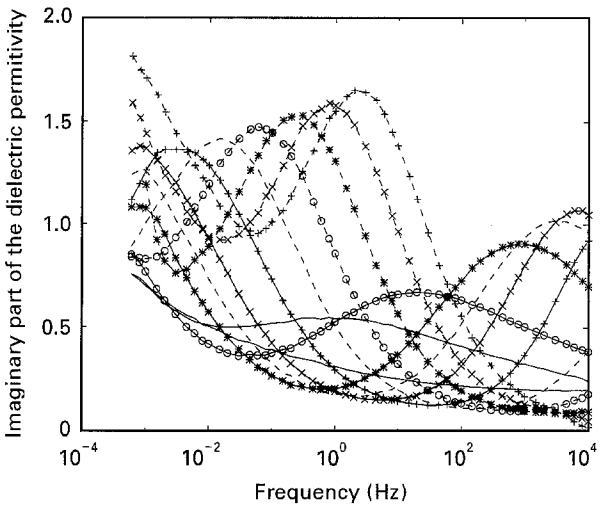

Figure 9 The variation of the imaginary part of the dielectric permittivity with frequency for PVDF between − 45 and + 40 °C, cf. Fig. 4. (——) − 45, (–O–) − 40, (–*–) − 30, (–×–) − 20, (–+–) − 10, (– – –) 0, (– – O – –) 10, (– – * – –) 20, (– – × – –) 30, (– – + – –) 40 °C.

− 20 to + 110 °C. For the α_a relaxation 38 kcal mol^{-1} was obtained. These values are in good agreement with results reported by Hedvig [6]. The data for these calculations were obtained in the same way as with the above polymers.

6. Discussion and conclusion

The results presented here support and extend previous work [1, 2] on the dipole response of the solid polymeric materials poly(methyl methacrylate) (PMMA) and nitrile butadiene rubber (NBR). In particular, also in the present study of PA6, PVC, EVA copolymer and PVDF, the dipole relaxation contribution to the dielectric response could be separated from the conductivity contribution at least for the lower temperatures. However, this separation and analysis is not exact, for both experimental and theoretical reasons.

The normalized inflexion slopes, $F_d/\Delta C$, of the experimental curves were evaluated graphically and by fitting a modified KWW or stretched exponential function to the data. In the main the two methods gave quite similar results. One should bear in mind that both methods make use of the same (graphically determined) ΔC and therefore are not completely independent. Thus ΔC, which cannot be determined exactly by the graphical method, plays a central role here. Further, stretched exponentials are not the only functions which can be used to fit the dipole relaxation parts of the curves, and the conductivity parts of the curves cannot be exactly linear indefinitely. Ideally, an analytical theory for the whole response is required, but such a theory does not exist at the present time.

An alternative approach to analysing the data is to use Cole–Cole or related diagrams (Davidson–Cole diagrams or Havriliak–Negami diagrams) to describe the relaxation quantitatively [7]. Havriliak–Negami diagrams can be fitted to our data in the frequency domain in an *ad hoc* fashion, giving results equivalent to our fits of the extended exponential in the time-domain data. We agree with Boyd *et al.* [7] that the Havriliak–Negami equation in the frequency domain and the stretched exponential in the time-domain are about equally good as a means of fitting analytical functions to data, but we find that the stretched exponential is more useful in the present work.

In spite of these difficulties, the experimental results can be summarized as follows. At the lowest temperatures used in this study, typically below − 20 °C, the normalized inflexion slope approaches 0.1, which value is characteristic of highly cooperative relaxation or a strong "connectedness" of the relaxing dipole groups involved. As the temperature is raised the "connectedness" is disrupted and $F_d/\Delta C$ approaches $1/e$ (β/e with $\beta = 1$), the Maxwellian response of independent dipoles.

What would have happened if much lower temperatures had also been investigated? It is reasonable to predict that $F_d/\Delta C$ would have remained near 0.1, judging by the temperature dependence of $F_d/\Delta C$ for PVC or for PMMA [1, 2].

At the other extreme, what would have happened for higher temperatures than those studied here? On theoretical grounds it is deemed unlikely that $F_d/\Delta C$ would have exceeded $1/e$ significantly, that is, if the dipole response could be separated from the conduction contribution.

In the end, the temperatures for which $F_d/\Delta C$ remains near 0.1 or for which it approaches $1/e$, are of interest as they could characterize the dipole groups dominating the relaxation. A simple comparison of these characteristic temperatures to the glass transition temperatures, T_g, of the various polymers is not fruitful. A more sophisticated analysis of this question is necessary in order to understand these results completely.

Finally, activation energies obtained from the temperature dependence of the imaginary dielectric constant are in agreement with previously published independent results. This experimental check on the accuracy of the data and analysis is encouraging.

Acknowledgement

The authors thank the Swedish Research Council for Engineering Science for financial support of this work.

References

1. M. SAFARI ARDI, W. DICK and J. KUBÁT, *Coll. Polym. Sci.* **271** (1993) 739.
2. *Idem*, in IEE Sixth International Conference on "Dielectric Materials, Measurements and Applications", IEE Conference Publication (IEE London) **363** (1992) p. 476.
3. J. KUBÁT and M. RIGDAHL, in "Failure of Plastics" edited by W. Brostow and R. D. Corneliussen (Hanser, Munich 1986) p. 60.
4. C. P. LINDSEY and G. D. PATTERSON, *J. Chem. Phys.* **73** (1980) 3348.
5. N. G. McCRUM, B. E. READ and G. WILLIAMS, "Anelastic and Dielectric Effects in Polymeric Solids" (Wiley, New York 1967).
6. P. HEDVIG, "Dielectric Spectroscopy of Polymers" (Hilger, Bristol, 1977) p. 229.
7. R. H. BOYD, R. W. DEVEREAUX and R. B. THAYER, *Polym. Preprints* **31** (1990) 279.

Received 12 January
and accepted 22 June 1995